Cell Cycle 12:9, 1371–1384; May 1, 2013; © 2013 Landes Bioscience

Cancer metabolism, stemness and tumor recurrence

MCT1 and MCT4 are functional biomarkers of metabolic symbiosis in head and neck cancer

Joseph M. Curry,[1,‡,*] Madalina Tuluc,[2,‡] Diana Whitaker-Menezes,[3] Julie A. Ames,[1] Archana Anantharaman,[4] Aileen Butera,[5] Benjamin Leiby,[6] David M. Cognetti,[1] Federica Sotgia,[3,7,†] Michael P. Lisanti[3,7,†,*] and Ubaldo E. Martinez-Outschoorn[3,*]

[1]Department of Otolaryngology; Thomas Jefferson University; Philadelphia, PA USA; [2]Department of Pathology; Thomas Jefferson University; Philadelphia, PA USA; [3]Kimmel Cancer Center; Thomas Jefferson University; Philadelphia, PA USA; [4]Department of Medicine; Thomas Jefferson University; Philadelphia, PA USA; [5]Jefferson Medical College; Thomas Jefferson University; Philadelphia, PA USA; [6]Department of Pharmacology and Experimental Therapeutics; Division of Biostatistics; Thomas Jefferson University; Philadelphia, PA USA; [7]University of Manchester; Institute of Cancer Sciences; Breakthrough Breast Cancer Research Unit; Manchester, UK

[†]Current affiliation: Breakthrough Breast Cancer Research Unit; Institute of Cancer Sciences; University of Manchester; Manchester, UK

[‡]These authors contributed equally to this work.

Keywords: head and neck cancer, tumor recurrence, oxidative stress, stem cells, mitochondria, OXPHOS, glycolysis, monocarboxylate transporters (MCT), MCT1, MCT4, metabolic symbiosis, TOMM20, tumor stroma

Here, we interrogated head and neck cancer (HNSCC) specimens (n = 12) to examine if different metabolic compartments (oxidative vs. glycolytic) co-exist in human tumors. A large panel of well-established biomarkers was employed to determine the metabolic state of proliferative cancer cells. Interestingly, cell proliferation in cancer cells, as marked by Ki-67 immunostaining, was strictly correlated with oxidative mitochondrial metabolism (OXPHOS) and the uptake of mitochondrial fuels, as detected via MCT1 expression ($p < 0.001$). More specifically, three metabolic tumor compartments were delineated: (1) proliferative and mitochondrial-rich cancer cells (Ki-67+/TOMM20+/COX+/MCT1+); (2) non-proliferative and mitochondrial-poor cancer cells (Ki-67–/TOMM20–/COX–/MCT1–); and (3) non-proliferative and mitochondrial-poor stromal cells (Ki-67–/TOMM20–/COX–/MCT1–). In addition, high oxidative stress (MCT4+) was very specific for cancer tissues. Thus, we next evaluated the prognostic value of MCT4 in a second independent patient cohort (n = 40). Most importantly, oxidative stress (MCT4+) in non-proliferating epithelial cancer cells predicted poor clinical outcome (tumor recurrence; $p < 0.0001$; log-rank test), and was functionally associated with FDG-PET avidity ($p < 0.04$). Similarly, oxidative stress (MCT4+) in tumor stromal cells was specifically associated with higher tumor stage ($p < 0.03$), and was a highly specific marker for cancer-associated fibroblasts ($p < 0.001$). We propose that oxidative stress is a key hallmark of tumor tissues that drives high-energy metabolism in adjacent proliferating mitochondrial-rich cancer cells, via the paracrine transfer of mitochondrial fuels (such as L-lactate and ketone bodies). New antioxidants and MCT4 inhibitors should be developed to metabolically target "three-compartment tumor metabolism" in head and neck cancers. It is remarkable that two "non-proliferating" populations of cells (Ki-67–/MCT4+) within the tumor can actually determine clinical outcome, likely by providing high-energy mitochondrial "fuels" for proliferative cancer cells to burn. Finally, we also show that in normal mucosal tissue, the basal epithelial "stem cell" layer is hyper-proliferative (Ki-67+), mitochondrial-rich (TOMM20+/COX+) and is metabolically programmed to use mitochondrial fuels (MCT1+), such as ketone bodies and L-lactate. Thus, oxidative mitochondrial metabolism (OXPHOS) is a common feature of both (1) normal stem cells and (2) proliferating cancer cells. As such, we should consider metabolically treating cancer patients with mitochondrial inhibitors (such as Metformin), and/or with a combination of MCT1 and MCT4 inhibitors, to target "metabolic symbiosis."

Introduction

Normal oral mucosa is highly organized and contains three morphologically distinct compartments. These include: (1) an underlying connective tissue layer; (2) a middle or basal layer of proliferating stem cells; and (3) an upper layer of differentiating squamous epithelia. Here, we investigated if this organization also represents a form of metabolic compartmentation, using a

*Correspondence to: Joseph M. Curry, Michael P. Lisanti and Ubaldo E. Martinez-Outschoorn; Email: joseph.curry@jefferson.edu, michaelp.lisanti@gmail.com and ubaldo.martinezoutschoorn@jefferson.edu
Submitted: 02/18/13; Accepted: 02/23/13
http://dx.doi.org/10.4161/cc.24092

Table 1. Metabolic biomarkers used for identifying cell proliferation, mitochondrial metabolism and oxidative stress

Biomarker	Status of metabolic function
Ki-67	Cell proliferation
TOMM20	Mitochondrial mass and oxidative mitochondrial metabolism (OXPHOS)
COX	Oxidative mitochondrial metabolism (OXPHOS)
MCT1	Uptake of mitochondrial fuels (L-lactate and ketone bodies)
MCT4	Oxidative stress, hypoxia, glycolysis and/or mitochondrial dysfunction; Production and export of mitochondrial fuels (L-lactate and ketone bodies)
LDHB	Glycolysis

panel of metabolic biomarkers. We also interrogated a series of head and neck squamous cell carcinomas (HNSCC) to examine similarities and differences in metabolic organization between normal mucosa and cancer mucosa.

Tumorigenesis in head and neck squamous cell carcinoma (HNSCC) is known to be driven by signaling pathways such as EGFR, p53, p16, IGFR, cyclin D1, HPV-E6-E7, PI3K-AKT-mTOR, NFkB and HIF-1α.[1] There is great interest in characterizing the links between signaling pathways and metabolism, but very little is known about the role of metabolism in tumorigenesis, treatment failure and recurrence risk in HNSCC.

Cancer cells have high bioenergetic requirements needed to maintain cell growth. Glycolysis with generation of lactate and reduced mitochondrial oxidative phosphorylation metabolism (OXPHOS) is commonly found in carcinoma cells in culture.[2-5] OXPHOS generates more ATP per molecule of glucose than glycolysis with lactate generation and hence it is unclear why some cells would use a metabolically inefficient pathway. It has been hypothesized that glycolysis may confer a growth and survival advantage, although the mechanism is unknown.[2,6,7] It should be noted that there is great heterogeneity in cancer metabolism, and differences in metabolism are observed depending on experimental conditions and particularly if homotypic culture experiments are performed, compared with co-culture experiments or in situ tumor analyses.[7-10]

More recently, a two-compartment view of tumor metabolism has been proposed using Paget's "seed and soil hypothesis" that may explain intra and inter-tumoral metabolic heterogeneity. Cancer cells require a rich, metabolically permissive microenvironment to promote tumor growth and metastasis.[10-12] In this metabolic model, carcinoma cells secrete hydrogen peroxide to induce oxidative stress in tumor fibroblasts or stromal cells.[13] These fibroblasts then increase their production of reactive oxidative species (ROS), which induces aerobic glycolysis and autophagy and results in increased levels of intermediate catabolites such as lactate, glutamine and ketone bodies.[10] The fibroblasts release these catabolites into the tumor microenvironment, stimulating mitochondrial biogenesis and OXPHOS in carcinoma cells.[14-16] Metabolic coupling with glycolysis in some cells and OXPHOS metabolism in other epithelial cancer cells promotes proliferation and resistance to apoptosis.[17]

Most studies on HNSCC cell metabolism suggest that these carcinoma cells are glycolytic with high L-lactate generation. These metabolic studies have been performed with either homotypic cell culture experiments or whole section analyses, but no in situ tumor mitochondrial metabolic studies have been performed to our knowledge. High tumor lactate concentrations in HNSCC are associated with subsequent nodal and distant metastases.[18,19] Most HNSCC cells generate significantly higher levels of lactate compared with normal human oral keratinocytes (NHOK), although several cell lines generate significantly lower lactate levels than NHOKs.[20] It has been postulated that the cells with decreased lactate levels have high lactate uptake via monocarboxylate transporters (MCTs), and this allows them to generate large amounts of ATP via OXPHOS.[20] The majority of HNSCC cell lines in homotypic culture were glycolytic and had decreased mitochondrial activity with a reduction in mitochondrial membrane potential.[21] When deprived of glucose, these cell lines showed a substantial increase in early and late apoptosis. However, when the cells were supplemented with excess pyruvate, some of the effects were reversed, which suggests that OXPHOS is important to support HSNCC cell proliferation in the presence of a catabolite-rich microenvironment.[21] In summary, recent studies suggest that metabolic heterogeneity and metabolic coupling occur in HNSCC.

The goal of this study was to evaluate mitochondrial and glycolytic metabolism in HNSCC tumor compartments. Normal squamous mucosa (NM) is compartmentalized, with the basal layer having high proliferative rates, while the well-differentiated epithelial cells have low proliferative rates. This compartmentalization is frequently observed in HNSCC, where poorly differentiated highly proliferative carcinoma cells coexist with well differentiated-low proliferative carcinoma cells.

We used a panel of biomarkers to assess metabolic compartmentation in HNSCC primary tumors (**Table 1**). Mitochondrial metabolism was determined by studying cytochrome C oxidase (COX) activity, expression of TOMM20 and MCT1. COX is the terminal enzyme in the mitochondrial electron transport chain required for oxidative phosphorylation to generate ATP.[9] COX activity is a surrogate marker for mitochondrial respiration or OXPHOS metabolism.[22-25] Low COX activity is the gold standard to diagnose human myopathies and neurologic diseases due to mitochondrial dysfunction.[26-29] TOMM20 is a protein found in the outer mitochondrial membrane, which recognizes and sorts precursor proteins in the cytosol (i.e., translocase) that are crucial to the biogenesis of mitochondria.[30,31] TOMM20 expression correlates with mitochondrial mass and OXPHOS metabolism.[32] Monocarboxylate transporters are a family of membrane proteins (MCT) that demonstrate proton-linked passive symport of lactate, pyruvate and ketone bodies

into and out of cells.[33] MCT1 is ubiquitously expressed in multiple cell types and cancer cell lines.[6,33,34] It is upregulated and expressed most prominently in cells with increased mitochondrial OXPHOS, such as heart and red muscle, suggesting an important role in lactic acid and ketone body oxidation.[33,35] MCT4 is the main transporter of lactate out of cells, it also exports ketone bodies out of cells and is a marker of oxidative stress.[33,36-38] The expression of MCT4 is upregulated by HIF-1α, which is the main glycolytic transcription factor induced by oxidative stress and hypoxia.[38,39] Oxidative stress and hypoxia are known markers for aggressive behavior in a variety of tumors, but few biomarkers have been identified.[40-45] Lactate dehydrogenase-B (LDHB) is an isoform of LDH and a marker of glycolysis.[46,47]

Results

Here, we used a panel of biomarkers to assess metabolic compartmentation in HNSCC primary tumors (**Table 1**).

Baseline characteristics of the cross-sectional group and retrospective cohort. Average age at the time of diagnosis for the cross-sectional group of 12 subjects was 63.3 y (range 50–81-y-old), and in the retrospective cohort of 42 subjects, 60.7 y (range 36–83-y-old). Three patients had oral cavity primary lesions, seven had oropharyngeal, one had hypopharyngeal, and one had laryngeal primary lesions in the cross-sectional group, while as all patients had oral cavity primary lesions in the retrospective cohort. Ten subjects in the cross-sectional group had clinical and radiologic stage IV disease, with nine having N2 disease, and 21 subjects in the retrospective cohort had stage IV disease. Two patients in the cross-sectional group had clinical and radiologic stage III disease, with one having N1 nodal disease, and nine subjects in the retrospective cohort had stage III disease. Nine of these subjects had primary surgical resection, and the remaining three were treated with chemo-radiotherapy. Remaining clinical and pathologic factors are detailed in **Table 2**.

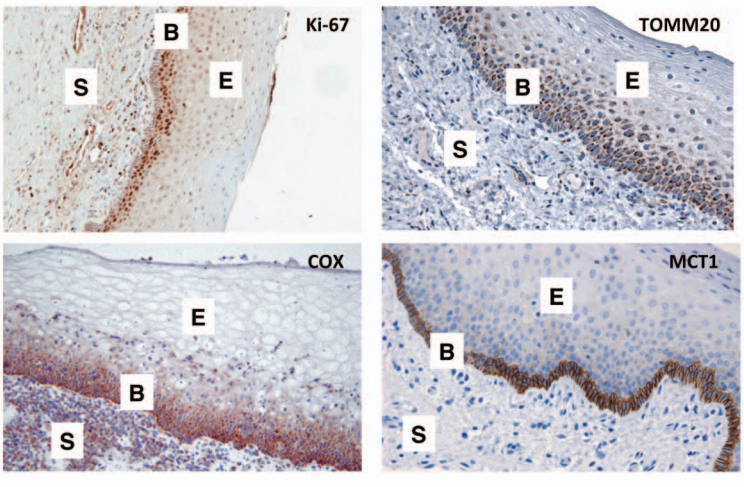

Figure 1. Distribution of proliferative and mitochondrial biomarkers in normal mucosa. Normal mucosal tissue was subjected to staining (brown color) with a variety of metabolic markers. Note that the basal "stem cell" layer is highly enriched in markers of proliferation (Ki-67), oxidative mitochondrial metabolism (TOMM20 and COX) and L-lactate/ketone body utilization (MCT1). Based on these studies, MCT1 is a highly selective marker of the basal stem cell layer. S, underlying connective tissue layer; B, basal stem cell layer; E, differentiating squamous epithelial layer. Original magnification: 20× (Ki-67 and COX); 40× (TOMM20 and MCT1).

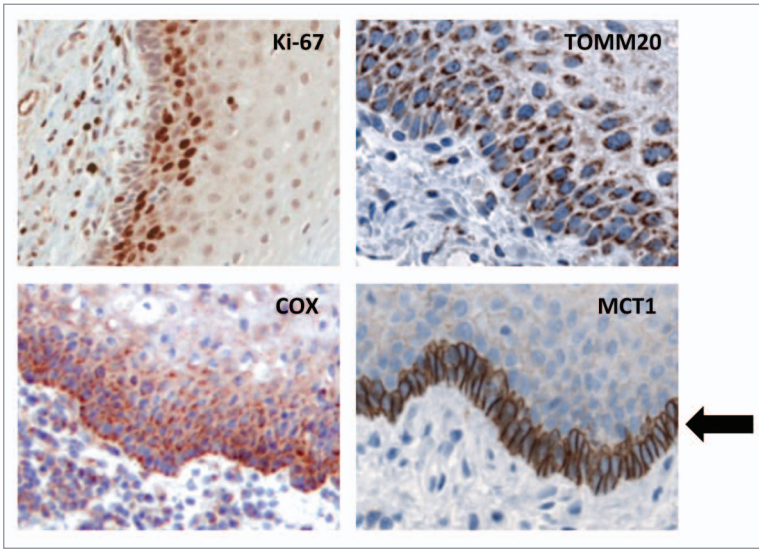

Figure 2. MCT1 is a specific marker for basal stem cells, and co-distributes with markers of proliferation (Ki-67) and mitochondrial metabolism (TOMM20 and COX). As in **Figure 1**, except that selected areas are shown at a higher magnification to better appreciate the staining of the basal stem cell layer. An arrow points at MCT1 staining, which is a specific marker for basal stem cells.

The normal basal stem cell layer is associated with high L-lactate and ketone body uptake and mitochondrial metabolism: MCT1 is a highly selective basal stem cell marker. Mitochondrial metabolism and the status of uptake of lactate and ketone bodies in normal mucosa were evaluated. Adjacent sections were used to assess proliferation, mitochondrial OXPHOS and lactate uptake. The basal layer has the highest proliferation rate on the basis of Ki-67 staining (**Fig. 1**, left upper panel). TOMM20 is a mitochondrial transport protein whose expression correlates with mitochondrial respiration. TOMM20 exhibits cytoplasmic staining, with a granular pattern. We considered positive all cells in which the majority of the cytoplasm demonstrated strong granular staining. The bottom third of epithelia adjacent to the dermis has the highest staining for TOMM20 (**Fig. 1**, right upper panel). To confirm that the TOMM20 staining pattern was staining functionally active mitochondria, we next performed the COX assay. The COX assay is a direct measure of mitochondrial complex IV activity in situ and is performed directly on unfixed frozen tissue sections. COX staining is cytoplasmic, with a diffuse pattern. The COX staining pattern is very similar to that of TOMM20 and similar cell populations to those that stain for

Table 2. Baseline characteristics and adjuvant treatments

Demographics/features	Cross-sectional group (n = 12)			Retrospective cohort (n = 42)		
Sex	m 10/f 2			m 27/f 15		
Mean age (yr)	63.3 (50–81)			60.7 (42–84)		
Tobacco use	11 (8*)			30 (12*)		
Alcohol use	7 (4*)			27(20*)		
Mean followup (mo)	8.6 (1–9.3)			45 (2.8–94.9)		
Subsite						
Larynx	1					
Oropharynx	7					
Hypopharynx	1					
Oral cavity	3			42		
Oral tongue	3			28		
Buccal				1		
Lip				1		
FOM				9		
RMT				3		
Differentiation						
Well-moderate	8			40		
poor	4			2		
Prognostic factors	(+)	(–)	ND	(+)	(–)	ND
PNI	3	5	4	16	24	2
LVI	3	5	4	14	26	4
ECS†	4	5	3	3	9	8
p16	5	5	2	1	27	14
Surgical margins	1	7	4	1**	41	
Adjuvant treatment	(+)	(–)	ND	(+)	(–)	ND
Primary surgery	9	3	0	42	0	0
XRT	8	4	0	29	8	5
Systemic Rx	6	6	0	21	15	6

Baseline characteristics including demographics, tumor subsites, pathologic factors and adjuvant treatments are described, for the cross-sectional group and retrospective cohort. †ECS is determined only for node-positive subjects in the retrospective cohort, n = 20. ND, not determined; *,previous tobacco or alcohol use, but have quit for over 3 y; **, initially margins were positive but underwent re-resection to negative margins 1 wk later.

TOMM20, show strong COX activity and are found in the lower third of the epidermis (**Fig. 1**, left lower panel). MCT1 expression correlates with lactate and ketone body uptake and utilization for OXPHOS metabolism. The basal layer, which is where squamous epithelia stem cells and highly proliferative cells are located, has high membrane MCT1 staining (**Fig. 1**, right lower panel). In fact, MCT1 gave the most specific staining pattern for the basal layer when compared with TOMM20 and COX histochemical activity. After this characterization of mitochondrial metabolism in normal mucosa, we next set out to characterize it in HNSCC mucosa.

Thus, we conclude that the highly proliferative basal stem cell layer of normal mucosa is mitochondrial-rich and is specialized for the use of mitochondrial fuels, such as L-lactate and ketone bodies. As such, MCT1 may be a novel stem cell marker. Higher power views are also shown (**Fig. 2**) to better appreciate staining in the basal stem cell layer.

High OXPHOS metabolism and evidence of lactate and ketone body import is present in highly proliferative epithelial cancer cell populations. Adjacent sections were used to assess proliferation, mitochondrial OXPHOS and glycolysis within similar populations of tumor and stromal cells. Initially, samples were stained for Ki-67 to identify carcinoma cells, with relatively high and low proliferation rates.

In well-differentiated HNSCC, nests of well-differentiated carcinoma cells were surrounded by a rim of basaloid, less differentiated carcinoma cells (**Fig. 3**). These less differentiated carcinoma cells are described as the tumor leading edge and are found adjacent to the reactive stroma, which is primarily composed of fibroblasts and inflammatory cells. In well-differentiated tumors, Ki-67 showed a low proliferative index in the well-differentiated carcinoma cells in contrast with the poorly differentiated carcinoma cells of the leading edge, which showed the highest Ki-67 reactivity and were located at the stromal-epithelial interface.

Poorly differentiated HNSCC is composed of less differentiated carcinoma cells with enlarged and hyperchromatic nuclei with high N/C ratio and no keratin production arranged in irregular cords, small nests or individual cells (**Fig. 4**). The Ki-67 staining pattern in these poorly differentiated tumors showed a more uniform distribution, as compared with the stratification revealed by the Ki-67 pattern in the well-differentiated tumors.

We next focused our attention on TOMM20, whose expression correlates with mitochondrial respiration (**Fig. 5**, left panels). We were interested in evaluating the mitochondrial status of the different carcinoma cell populations and stromal cells. In well-differentiated tumors, TOMM20 expression was highest in the rapidly proliferating population of carcinoma cells of the leading edge in all samples examined, while the well differentiated carcinoma component showed low or absent reactivity. In the poorly differentiated tumors, expression of TOMM20 was uniform and strongly positive within all the carcinoma cells. In all 12 samples examined, TOMM20 expression was strongest in carcinoma cells, as compared with the adjacent stromal cell population.

To confirm that the TOMM20 staining pattern was staining functionally active mitochondria, we performed the COX assay (cytochrome C oxidase), which is a direct measure of mitochondrial complex IV activity. The highest COX activity was detected in carcinoma cells (**Fig. 6**), as compared with the adjacent stromal cells. Furthermore, in well-differentiated HNSCC samples, the highest mitochondrial activity was detected in the carcinoma cells of the leading edge, adjacent to the stroma, with the more differentiated carcinoma cells having lower activity. High-grade HNSCC showed strong COX activity in all of the carcinoma cells, similar to TOMM20.

Based on the TOMM20 staining pattern and COX activity assay, we wanted to study MCT1 expression, which correlates with lactate and ketone body uptake and utilization for OXPHOS metabolism. In positive cells, MCT1 exhibits a strong, circumferential complete membranous staining. We considered positive all cells in which the above pattern was present. In low grade HNSCC, the strongest MCT1 staining was in the highly proliferative, poorly differentiated carcinoma cell population, while the more differentiated carcinoma cell population of the tumors had low or absent staining (**Fig. 5**, right panels). In high-grade tumors, expression of MCT1 again showed a uniform and strongly positive distribution within the majority of the carcinoma cells. However, MCT1 expression was not detected in the stromal compartment (**Fig. 7**). In summary, the pattern of reactivity for MCT1 was similar to that of Ki-67, TOMM20 and COX. The IHC data for mitochondrial metabolism markers are summarized in **Table 3**.

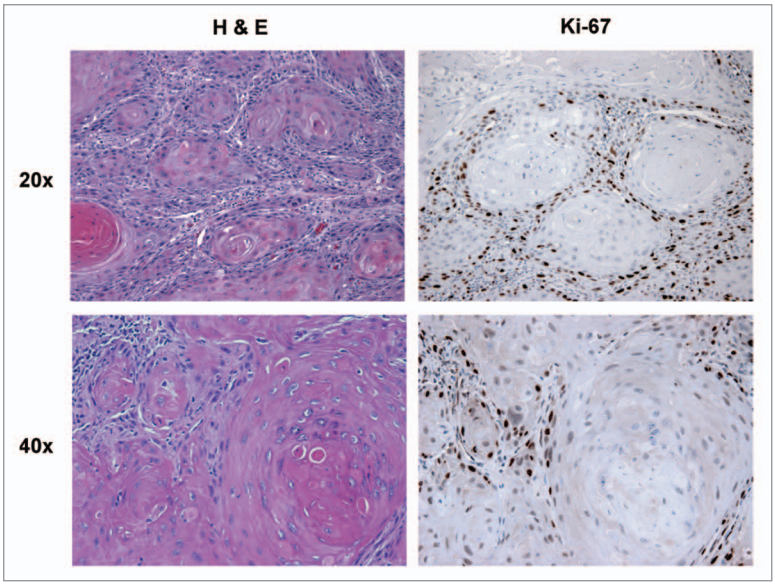

Figure 3. Morphology and proliferation in well-differentiated HNSCC tumor tissue: H&E and Ki-67 immunostaining. Note that carcinoma cells are more differentiated in the center of clusters or nests, with occasional keratin pearls. The carcinoma cells in the periphery of the nests stain strongly for Ki-67, which is absent in the center of the nests. Original magnification: 20× and 40×, as indicated.

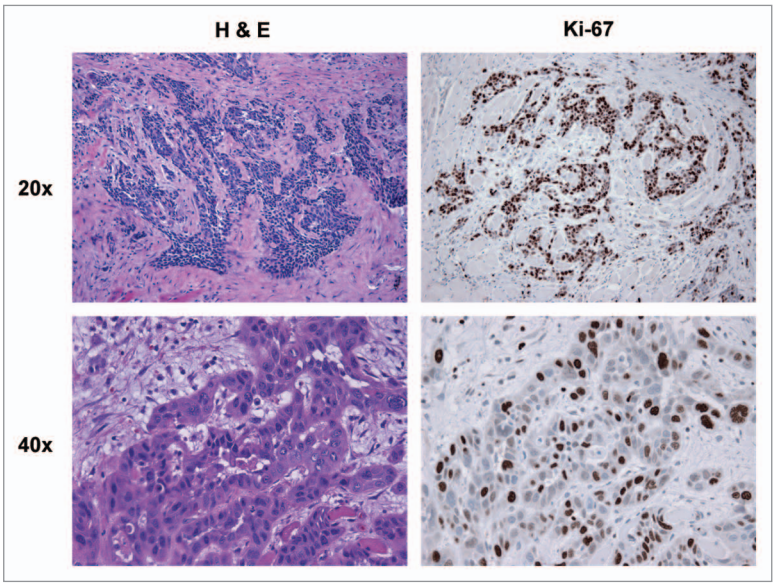

Figure 4. Morphology and proliferation in poorly differentiated HNSCC tumor tissue: H&E and Ki-67 immunostaining. Note that carcinoma cells form small clusters or nests without differentiation or keratin pearls. The carcinoma cells in the nests diffusely stain strongly for Ki-67. Note also that the tumor stroma is negative for Ki-67 staining. Original magnification: 20× and 40×, as indicated.

Based on this analysis, the cellular distribution of proliferative markers (Ki-67) strictly correlated with mitochondrial markers (TOMM20, COX and MCT1), indicating that the proliferative population of epithelial cancer cells must use oxidative mitochondrial metabolism (OXPHOS). This is analogous to our findings

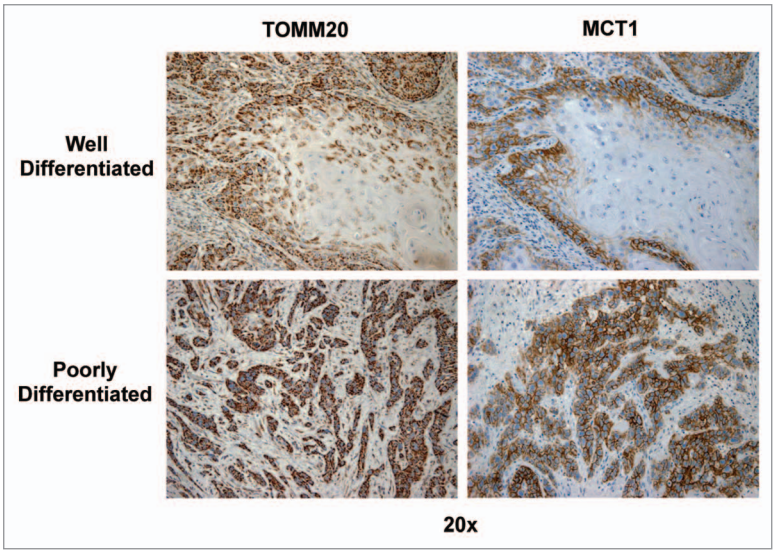

Figure 5. TOMM20 and MCT1 immunostaining in well-differentiated and poorly differentiated HNSCC specimens. In well-differentiated, note that carcinoma cells in the periphery of nests have high TOMM20 staining (brown), while well differentiated cells in the center of nests have low TOMM20 staining. In poorly differentiated, note that carcinoma cells in the nests strongly stain for TOMM20 (brown). Virtually identical results were obtained for MCT1, as well. Note also that the tumor stroma is negative for both TOMM20 and MCT1-staining. Original magnification: 20×, as indicated.

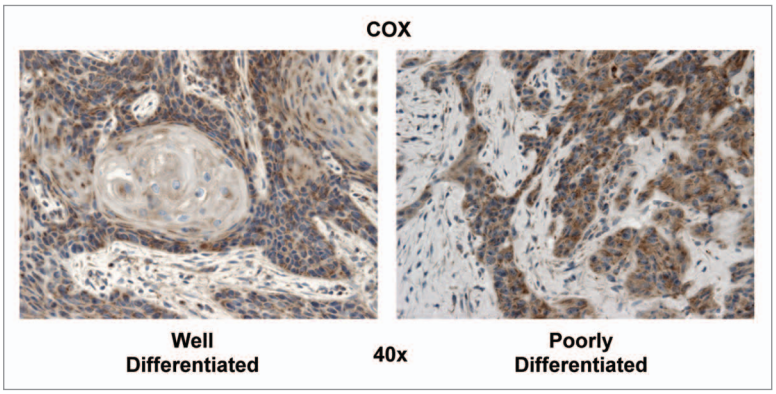

Figure 6. COX mitochondrial activity staining in well-differentiated and poorly differentiated HNSCC specimens. In well-differentiated, note that carcinoma cells in the periphery of nests have high COX activity (brown), while as differentiated cells in the center of nests have low COX activity. In poorly differentiated, note that carcinoma cells in the nests diffusely stain strongly for COX. Note also that the tumor stroma is negative COX staining. Original magnification: 40×, as indicated.

with the basal stem cell layer in normal mucosal tissue, and is consistent with the "cancer stem cell hypothesis."

Cancer-associated fibroblasts (CAFs) highly express MCT4, a specific marker of oxidative stress, glycolytic metabolism and L-lactate/ketone body export. Fibroblasts located in cancer mucosa, which are in close proximity to carcinoma cells, are here defined as cancer-associated fibroblasts (CAFs). CAFs were relatively negative for TOMM20 expression and COX activity, as compared with the highly proliferative carcinoma cells, in all 12 samples, and CAFs were negative for MCT1 (**Figs. 3–7**). Ki-67 staining was very low or absent in CAFs and normal fibroblasts (NFs), and no differences were appreciated (data not shown).

We were also interested in evaluating glycolysis and oxidative stress in the highly proliferative carcinoma cell compartment and in carcinoma cells with low proliferation rates. Hence, we evaluated the expression of two proteins associated with glycolytic energy production and oxidative stress, MCT4 and LDH-B. MCT4 expression is also a marker of lactate and ketone body export out of cells. Strong MCT4 immunoreactivity was found in the majority of well-differentiated carcinoma cells and CAFs (**Figs. 8 and 9**). In contrast, MCT4 staining in normal fibroblasts was absent in all samples that contained adjacent normal stromal areas. The strongest LDH-B expression was found in CAFs, while there was low to absent expression in the carcinoma cells (**Fig. 10**).

Retrospective analysis of MCT4 in OSCC. To further evaluate the relationship of MCT4 expression in CAFs, as compared with NFs, we expanded our cohort to include 42 additional OSCC subjects. Forty out of the 42 subjects had evaluable normal mucosa as well as cancer mucosa. MCT4 staining was performed in these additional samples, and the expression of MCT4 in CAFs and NFs was scored. In all 40 evaluable additional samples, MCT4 expression in NFs was minimal or absent (**Fig. 11**), while 26 of the 40 subjects had positive MCT4 expression in CAFs (**Table 4**).

Fifty percent of patients had stage IV disease (21/42), 11 patients had stage III, six patients had stage II, and four patients had stage I (**Table 5**). One patient had a negative frozen margin, which was positive on final path and underwent re-resection to negative final margins. The mean duration of follow-up was 31 mo (**Table 2**). High stromal MCT4 (> 30% stromal cells staining for MCT4) was associated with higher stage disease ($p = 0.034$) (**Table 7**). More specifically, stage III or IV disease was present in 22 out of 26 subjects with high stromal MCT4 expression, while only eight out of 16 subjects with low MCT4 expression had stage III or IV disease (**Table 5**). The majority of tumors had high stromal MCT4 and low epithelial MCT4 (26 out of 42 tumors had high stromal MCT4 and 26 out of 42 had low epithelial MCT4).

Clinical outcomes were assessed according to MCT4 epithelial staining as well. A statistically significant decrease in disease-free survival (DFS) was identified, with a large MCT4-positive carcinoma compartment (> 25% carcinoma cells staining for MCT4) in univariable and multivariable analysis (**Table 6**). Kaplan-Meier analysis is shown in **Figure 12** ($p < 0.0001$; log-rank test), illustrating a clear association with lower disease-free survival, which is indicative of high tumor recurrence. Perineural invasion (PNI) correlated with a large MCT4-positive carcinoma compartment (**Table 7**). Finally, the SUV reported on ^{18}FDG PET/CT was assessed with respect to MCT4

Table 3. Markers of mitochondrial metabolism in HNSCC: Epithelial vs. stromal compartments

Morphologic compartment	Total	COX†		TOMM20†		MCT1†	
		Low/absent	High	Low/absent	High	Low/absent	High
Leading edge/poorly differentiated carcinoma cells High proliferation: Ki-67(+)	12	0	12	0	12	2	10
Well-differentiated carcinoma cells Low proliferation:Ki-67(–)	8	8	0	8	0	8	0
CAFs	12	12	0	12	0	12	0
NFs	9	9	0	9	0	9	0

Staining for markers of proliferation (Ki-67) and mitochondrial metabolism (COX, TOMM20 and MCT1) was performed on the samples from subjects in the cross-sectional group. Staining was assessed in two types of carcinoma cells: the leading edge/poorly differentiated carcinoma cells (12 samples were evaluable) and in the well differentiated carcinoma cells (8 samples were evaluable). Staining was also assessed in two types of fibroblasts: cancer-associated fibroblasts (CAFs) (12 samples were evaluable) and normal fibroblasts (NFs) (9 samples were evaluable). †Fisher's exact test for comparison of COX, TOMM20 and MCT1 expression in leading edge/poorly differentiated carcinoma cells vs. well differentiated carcinoma cells, $p < 0.001$ for all three comparisons.

expression, and a large MCT4-positive carcinoma compartment correlated with greater SUV (**Table 7**). However, pathologic and nodal staging, as well as lymphovascular invasion (LVI), did not correlate with the percentage of epithelial cells staining for MCT4 (**Table 6**).

As MCT4 is a tumor-specific marker of oxidative stress, glycolysis and hypoxia in non-proliferating epithelial cancer cells and tumor stromal cells, our data directly show how non-proliferating cells that are undergoing oxidative stress can metabolically contribute to tumor growth and poor clinical outcome.

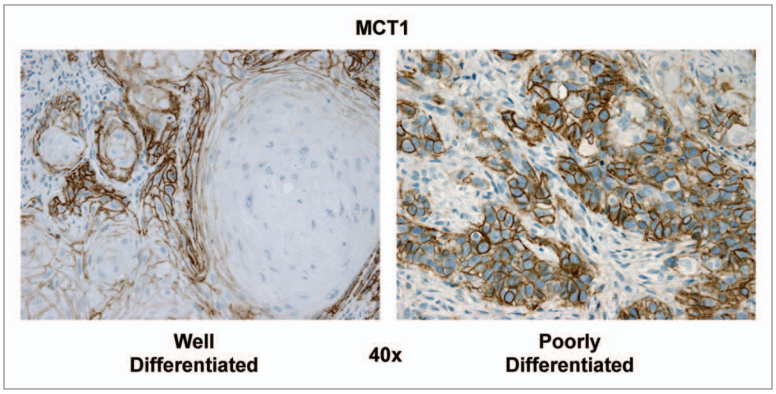

Figure 7. Higher power views of MCT1 immunostaining in HNSCC specimens. As in **Figure 5**, except higher power view are shown to better appreciate the plasma membrane staining of MCT1+ tumor cells. Also, note that MCT1 staining is absent from the the tumor stroma and cancer-associated fibroblasts. Original magnification: 40×, as indicated.

Discussion

Here, we present new evidence that both normal mucosa and head and neck cancers are divided into three separate metabolic compartments (**Figs. 13 and 14**). Based on our biomarker analysis, in the normal basal stem cell layer, the proliferative stem cells (Ki-67+) are mitochondrial-rich (TOMM20+/COX+) and are specialized to use L-lactate and ketone bodies as high-energy mitochondrial fuels (MCT1+). Similarly, in head and neck cancers, we detected a population of highly proliferative epithelial cancer cells that were rich in mitochondria and used mitochondrial fuels (TOMM20+/COX+/MCT1+). These proliferating cells were surrounded by non-proliferating tumor cells (epithelial and stromal) (Ki-67–), which were mitochondrial-deficient (TOMM20–/COX–/MCT1–), and were undergoing oxidative stress and glycolysis (MCT4+). Remarkably, this population of non-proliferating cells (MCT4+) had a striking effect on both tumor stage and clinical outcome. Thus, we postulate that the population of non-proliferating tumor cells may determine clinical outcome via a simple energy-transfer mechanism ("a lactate/ketone shuttle"), which we have termed three-compartment tumor metabolism (**Fig. 14**). In this model, non-proliferating tumor cells (stromal and epithelial) fuel the growth of proliferating tumor cells, via a form of metabolic symbiosis. As such, two catabolic non-proliferating compartments may fuel the expansion of the anabolic proliferative compartment. Interestingly, MCT4+ staining was specific for tumor tissue and was not detected in normal mucosa. Thus, oxidative stress appears to be a specific marker of carcinogenesis and correlates with high PET avidity and poor clinical outcome.

This study set out to characterize metabolism in normal mucosa and HNSCC mucosa in situ. Normal mucosa has the basal layer, where normal epithelial stem cells are located, is highly proliferative and non-differentiated. The basal layer gives rise to cells in the remainder of the epithelium. The basal layer of squamous epithelium shares features with squamous cell carcinoma cells, and it is now believed that squamous cell carcinomas of the head and neck derive from the basal layer.[48-51] Normal mucosa provides us an opportunity to identify stem cells topographically. We have discovered that MCT1, a marker of lactate and ketone body uptake, stains exclusively the basal layer in the normal mucosa that has high OXPHOS metabolism. HNSCC have carcinoma cells that appear similar to normal basal layer cells morphologically. We have discovered that these basal-like carcinoma cells also have the metabolic features of normal basal layer cells with high MCT1 expression, high OXPHOS and low glycolysis.

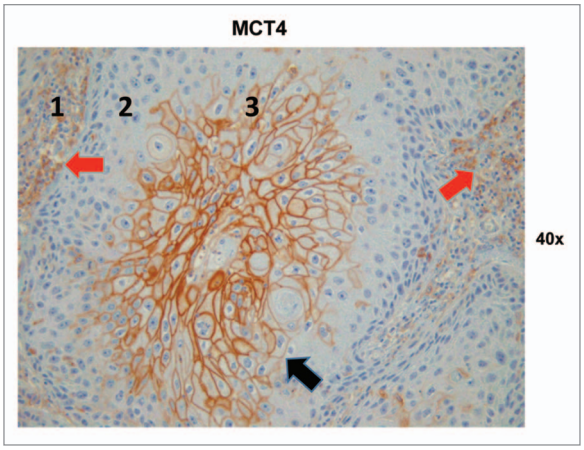

Figure 8. MCT4 epithelial immunostaining in HNSCC tumor tissue. Three different tumor regions or metabolic compartments are as indicated: (1) is the tumor stroma; (2) represents the proliferating cancer cell compartment; and (3) is the non-proliferating cancer cell compartment. Note that MCT4 staining is primarily localized to the tumor stroma (red arrows) and the non-proliferating epithelial cancer cell compartment (black arrow). Note also that the non-proliferating MCT4+ cancer cells appear enlarged or hypertrophic, which is consistent with a senescent phenotype. Original magnification: 40×, as indicated.

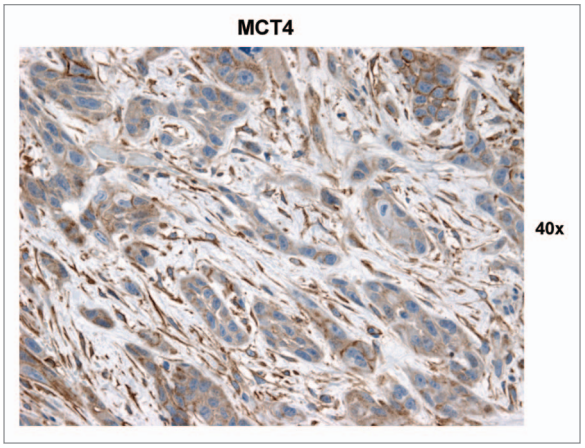

Figure 9. MCT4 stromal immunostaining in HNSCC tumor tissue. Note that the stromal cells separating nests of proliferating carcinoma cells have the highest MCT4 expression (brown). Original magnification: 40×, as indicated.

Table 4. MCT4 staining in normal fibroblasts (NFs) and cancer-associated fibroblasts (CAFs) in HNSCC

	NFs†	CAFs†
Low MCT4 staining	40	14
High MCT4 staining	0	26
Total cases	40	40

Staining for the lactate exporter and glycolytic marker MCT4 was performed on 40 samples from subjects in the retrospective cohort where morphologically normal mucosa was assessable. MCT4 staining was assessed in cancer-associated fibroblasts (CAFs) and normal fibroblasts (NFs). †Fisher's exact test for comparison of MCT4 expression in CAF vs. NF, $p < 0.001$.

This study links, for the first time in HNSCC, stemness with lactate and ketone body uptake and mitochondrial metabolism. The current results are consistent with a previous study showing that high lactate and ketone body levels in the microenvironment and uptake by carcinoma cells generates a stem-like gene expression signature in breast carcinomas.[52] Studies show that many non-transformed, rapidly proliferating cells have similar metabolic needs to those of cancer cells, and it is hypothesized that cancer cells revert to a metabolic phenotype reminiscent of rapidly dividing cells.[2,4] Our current study validates the idea that rapidly dividing HNSCC carcinoma cells share a mitochondrial metabolic phenotype (OXPHOS) with normal basal layer epithelial stem cells.

HNSCCs frequently have well differentiated epithelial and stromal cell compartments that have high MCT4 staining with low OXPHOS, high glycolysis, lactate and ketone body release out of cells and levels of oxidative stress (**Fig. 14**). MCT4 staining was found to be specific to the cancer tissues and absent from normal adjacent tissues. A significant subset of HNSCC tumors have a large glycolytic carcinoma cell compartment as measured by MCT4 expression and are associated with a statistically significantly decrease in DFS. It may be that these tumors are more aggressive, because they generate oxidative stress, lactate and ketone bodies to fuel mitochondrial metabolism (OXPHOS) in adjacent proliferating epithelial cancer cells with high MCT1 expression. MCT4 distinguishes normal fibroblasts (NFs) from CAFs, since MCT4 expression is absent in NFs, while it is high in CAFs in the majority of samples. Metabolic compartmentalization found here in HNSCC has been also described in breast, colon, ovarian and prostate cancers.[12,13,53-58]

OXPHOS as measured by COX activity and TOMM20 staining was present in the poorly differentiated compartment in all samples studied. These carcinoma cells with high OXPHOS had high proliferation rates and were prominent at the leading edge of the tumor in proximity to the stroma. It has been shown in lung cancer that high mitochondrial metabolism is necessary for cancer cell proliferation.[59] The more rapidly proliferating, poorly differentiated stem-cell like cancer cells are frequently the origin of metastasis.[60] Thus, high OXPHOS may be a marker for cells with metastatic potential and may be required for proliferation in HNSCC.

MCT1 is an importer of L-lactate and ketone bodies into cells, and high expression of MCT1 induces high OXPHOS and low glycolytic states.[6,61,62] We show here that MCT1 is the best marker of the basal stem cell layer of normal mucosa, and its expression correlates with high TOMM20 expression and COX activity in normal and cancer mucosa. Therefore, MCT1 is a possible metabolic therapeutic target in HNSCC, since our study shows increased expression in the most rapidly proliferating and metabolically active HNSCC cells. It is known that MCT1 expression is associated with poor outcomes in breast and gastric cancers.[63] Theoretically, inhibiting L-lactate and ketone body uptake by using MCT1 inhibitors could drastically reduce the supply of mitochondrial fuels to the most proliferative cell population(s), thereby diminishing OXPHOS and

ATP generation required for accelerated tumor growth and cell division. This would metabolically uncouple the highly proliferative cancer cells from less proliferative epithelial cancer and stromal cells, by forcing the highly proliferative cancer cells to rely on glycolysis as their primary source of ATP generation.[34,64] One potent MCT1 inhibitor, α-cyano-4-hydroxycinnamate (CHC), has anticancer effects in vitro and in vivo.[6,65] In vivo studies in mice showed that CHC significantly reduced tumor burden with minimal toxic effects.[6] Another MCT1 inhibitor, AZD-3965, is currently undergoing clinical trials and could be a therapeutic agent in HNSCC.[66] Studies to determine if other metabolic modulators are effective therapies for HNSCC also need to be performed. Metformin, which is a known mitochondrial OXPHOS inhibitor, is effective for both the prevention and treatment of HNSCC in vitro and in vivo.[67]

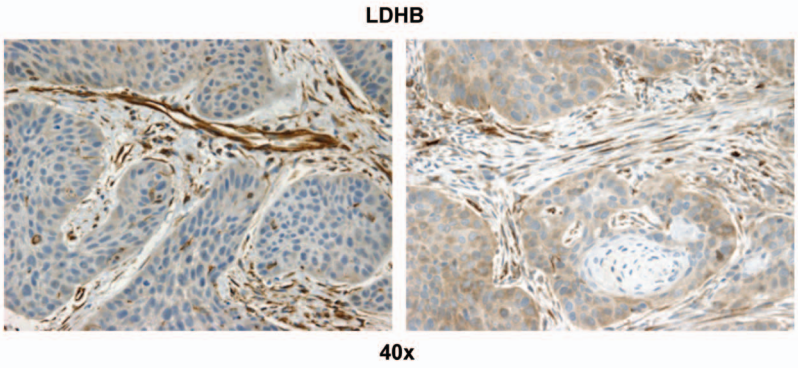

Figure 10. LDHB stromal immunostaining in HNSCC tumor tissue. Note that the stromal cells separating nests of proliferating carcinoma cells have the highest LDHB expression of all the cells in the sample (brown). Original magnification: 40×, as indicated.

There is a lack of clinically useful prognostic and predictive molecular markers in most HNSCC.[68] Our study shows that a large glycolytic carcinoma compartment with MCT4 expression is associated with shorter disease-free survival in OSCC and is functionally associated with high ^{18}FDG-PET SUV. MCT4 is a marker of glycolysis, lactate and ketone body release and oxidative stress.[38,69,70] The antioxidant N-acetyl cysteine (NAC) has been shown to decrease MCT4 expression and modulate metabolism.[53,54,71,72] Also, multiple medications have been shown to increase OXPHOS metabolism in vitro, such as carnitine, α-lipoic acid, vitamin C, riboflavin and B complex vitamins.[73] By increasing mitochondrial function in stromal cells and low proliferative epithelial cancer cells or decreasing the catabolite transfer, we may be able to disrupt metabolic coupling and induce tumor regression. Metabolic modulators should be investigated as potential therapies in HNSCC.

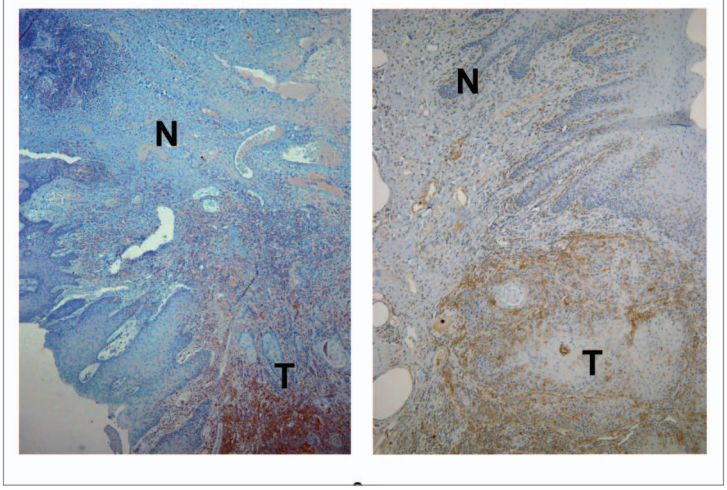

Figure 11. MCT4 immunostaining distinguishes tumor tissue from normal adjacent tissue. Note that MCT4 preferentially stains cancer-associated fibroblasts (CAFs) and not normal fibroblasts (NFs), allowing one to distinguish tumor tissue from normal tissue, even at low-magnification. Original magnification: 2×, as indicated. N, normal tissue; T, tumor tissue.

Altered metabolism is not only recognized as a hallmark of cancer cells and a possible therapy target, but FDG-PET scanning is an important diagnostic application.[8] ^{18}Fluoro-2 deoxy-glucose (FDG) is the radiotracer used in PET scans, since 2 deoxy-glucose is a competitive inhibitor of the rate-limiting glycolysis enzyme hexokinase.[74] FDG within cells cannot be metabolized and emits radiation.[75] FDG-PET-CT scans are almost always positive for HNSCC, and this has been considered evidence that this tumor type is glycolytic.[76,77] Here, we suggest that FDG-PET avidity in HNSCC is due to the MCT4+ non-proliferative carcinoma cells and CAFs. Higher SUV, which may require the presence of several metabolic compartments in HNSCC, is associated with advanced T stage and worse clinical outcome.[78-82] We show, as expected, that tumors with an expanded glycolytic carcinoma compartment have the highest FDG-PET avidity in HNSCC.

We have found that MCT4 expression is absent in the stroma in non-cancerous regions, and that in approximately 70% of cases, its expression increases in the tumor stroma. "Field cancerization" or "the field effect" describes the fact that non-cancerous tissues in proximity are at high risk of transformation in HNSCC due to epithelial dysplasia and its progression, although not due to direct invasion by carcinoma cells from the original tumor.[83-86] The field effect may be explained in part by the increased expression of MCT4 in stromal cells induced by proliferating epithelial cancer cells. This is consistent with observations in breast and ovarian cancer, where epithelial cancer cells have the ability to upregulate MCT4 expression in stromal cells at a distance, and high stromal MCT4 expression is associated with a poor prognosis.[53,54,72] Conversely, it is possible that high stromal MCT4 expression promotes transformation of non-cancerous epithelia. High carbonic anhydrase IX (CA IX) expression in the stroma, which is a marker of oxidative stress and glycolytic metabolism, is associated with a poor prognosis in HNSCC.[87,88] It is well established that HNSCC progresses through dysplasic stages and

Table 5. Staging, recurrence and death in retrospective HNSCC cohort

	Pathologic stage (TNM)					Recurrence			MCT4 epith.		MCT4 stromal (CAF)		MCT4 stroma (NF)	
Stage	**Total**	**N0**	**N1**	**N2**	**N3**	**LR**	**Dist.**	**Death**	**Low**	**High**	**Low**	**High**	**Low**	**High**
I	6	6				1	0	0	6 (1/0)	0 (0/0)	5 (1/0)	1 (0/0)	6	0
II	6	6				3	0	1	2 (0/0)	4 (3/1)	3 (2/0)	3 (1/1)	6	0
III	9	3	6			2	0	1	7 (1/1)	2 (1/0)	2 (1/1)	7 (1/0)	9	0
IV	21	7	0	14	0	7	2	7	11 (3/2)	10 (6/5)	6 (3/2)	15 (6/5)	19	0
Total	42	22	6	14	0	13	2	9	26 (5/3)	16 (10/6)	16 (7/3)	26 (8/6)	40*	0

Number of subjects who had loco-regional (LR) and distant (Dist.) recurrences as well as death are shown according to stage, nodal involvement and MCT4 staining in epithelial, CAF and NF compartments. In parenthesis are on the left side number of subjects who relapsed and on the right side are number of subjects who died. *Normal stroma was assessable in 40 subjects. NF, normal fibroblasts; CAF, cancer-associated fibroblasts.

Table 6. Correlation of epithelial MCT4 staining with disease-free survival

Disease-free survival (univariable analysis)	**Hazard ratio (95%CI)**	**p value**
MCT4 epithelial (high vs. low)	6.56 (2.32, 18.57)	**< 0.001**
Disease-free survival (multivariable analysis)	**Hazard ratio (95%CI)**	**p value**
MCT4 epithelial (high vs. low)	10.36 (2.56, 41.95)	**0.001**
Age at surgery	1.05 (0.996, 1.096)	0.07
Gender (M vs. F)	1.77 (0.49, 6.36)	0.38
Pathologic stage (1,2 vs. 3,4)	1.41 (0.23, 8.53)	0.71
Nodal stage: N0 vs. N+	3.62 (0.75, 17.48)	0.11

Univariable and multivariable models for overall survival were performed with epithelial MCT4 staining, age, gender, pathologic stage and nodal stage. N0, pathologically negative neck dissection; N+, pathologically positive neck dissection.

Table 7. Correlation of clinical and pathologic variables with MCT4 expression

Pathologic staging	**Spearman correlation coefficient**	**p value**
P Stage: MCT4 epithelial	0.209	0.18
P Stage: MCT4 stromal	0.328	**0.034**
N Stage: MCT4 epithelial	0.143	0.37
N Stage: MCT4 stromal	0.135	0.39
PNI and LVI	**p value (FE)**	
PNI: MCT4 epithelial	**0.018**	
PNI: MCT4 stromal	0.259	
LVI: MCT4 epithelial	0.328	
LVI: MCT4 stromal	0.177	
SUV on PET/CT	**p value (WMW)**	
SUV > 10: MCT4 epithelial	**0.038**	

Spearman correlation coefficients of epithelial and stromal MCT4 expression and staging, perineural invasion (PNI), lymphovascular invasion (LVI) and standard unit volume (SUV) on ^{18}FDG-PET are shown.

step-wise genetic changes,[89] but perhaps stromal oxidative stress and metabolism also modulate cancer progression.

Finally, advocates of the traditional Warburg effect have argued that aerobic glycolysis is required for the efficient proliferation of epithelial cancer cells, because it would shift a significant amount of metabolic precursors toward the generation of "biomass" to create new cancer cells.[3,66] However, little or no experimental data has been presented to validate this hypothesis in vivo.[7,90] Here, we show that "Warburg" cancer cells (MCT4+) are clearly non-proliferative (Ki-67–) and are mitochondrial-deficient (COX–/TOMM20–). Thus, aerobic glycolysis is not being used in vivo to "fuel" the proliferation of epithelial cancer cells. As a consequence, our data do not support the Warburg "biomass" and proliferation argument.

In summary, we show for the first time that metabolic compartmentalization exists in HNSCC mucosa, with highly proliferative epithelial cancer cells having high mitochondrial metabolism and lactate and ketone body uptake, while other non-proliferating carcinoma cells and CAFs have low mitochondrial metabolism, with high lactate and ketone body generation and high oxidative stress. This metabolic compartmentalization of HNSCC shares similarities with that of normal mucosa and likely drives proliferation via OXPHOS metabolism. We also show that MCT4 is a marker oxidative stress in non-proliferating cancer cells and CAFs, but it is absent in proliferating cancer cells and normal fibroblasts. Finally, high MCT4 expression is associated with higher tumor stage, PET avidity and poor clinical outcome. So, it is remarkable that the non-proliferating population of cells in the tumor actually determine clinical outcome.

Materials and Methods

Subjects. The protocol was approved by the Institutional Review Board at Thomas Jefferson University. Twelve subjects with a diagnosis of oral, oropharyngeal, hypopharyngeal or laryngeal HNSCC were enrolled in a cross-sectional study to evaluate metabolism in situ in surgical samples. Tumor samples were collected at the time of staging panendoscopy or definitive surgery and processed as described below.

Additionally, a retrospective chart and pathological review of subjects with a diagnosis of primary oral HNSCC (OSCC) between 2002 and 2010 was also performed. Immunohistochemical staining in this group was performed for MCT4. All included patients had no previous treatment and underwent primary treatment with surgical resection to negative margins. A total of 42 patients were included in the study. Patient data included age, sex, social history, tumor site, TNM stage, tumor morphology,

pre-operative imaging results, adjuvant treatment, length of follow up, recurrence and mortality. Patients were staged according to the American Joint Committee on Cancer (AJCC) guidelines. All patients underwent surgical resection of the primary lesion and neck dissection based on the clinical and radiologic findings. Postoperative treatment was based on the recommendation of the multidisciplinary tumor board, and adjuvant external beam radiotherapy and systemic therapy was used accordingly.

Sample processing. The first group of 12 samples was processed within 6 h of collection. Tumor samples were collected and snap frozen in OCT compound in liquid nitrogen and stored at -80°C. The remaining tumor was fixed in 10% formalin and paraffin embedded (FFPE) for hematoxylin and eosin (H&E) and immunohistochemistry staining (IHC).

The second group consisted of 42 subjects, for which archived FFPE tumor blocks were available. Sections of these blocks were used for H&E and IHC.

Paraffin immunohistochemistry. Five micron paraffin sections were prepared and stained with antibodies to Ki-67, TOMM20, MCT1, MCT4 and LDH-B. Ki-67 was from Abcam; MCT1 and MCT4 antibodies were the kind gift of Nancy J. Philp and have been described in detail;[91] MCT4 was also purchased from Santa Cruz Biotechnology; TOMM20 (F-10) was from Santa Cruz Biotechnology; LDHB was from Sigma-Aldrich. Briefly, sections were dewaxed, rehydrated through graded ethanols, and antigen retrieval was performed in 10 mM citrate buffer, pH 6.0, for 10 min using a pressure cooker. The sections were cooled, blocked with 3% hydrogen peroxide and then for endogenous biotin using the DakoCytomation Biotin BlocKing Sytem (Dako). Sections were next incubated with 10% goat serum for 30 min, followed by primary antibodies overnight at 4°C. Primary antibody binding was detected with a biotinylated species-specific secondary antibody (Vector Labs) followed by a streptavidin-horseradish peroxidase conjugate (Dako). Immunoreactivity was revealed with 3,3'-diaminobenzidine (Dako). Sections were counterstained with hematoxylin.

Epithelial and stromal staining patterns were studied and quantified independently. All tumor on a slide and its dominant staining pattern were considered when determining the percent of immune-positive carcinoma and stromal cells in a sample. The same pathologist scored all samples. An empirically derived scaling system was created based on evident staining patterns in the samples. An MCT4 epithelial staining score of low or high was given if < 25% or equal or greater than 25% of carcinoma cells stained positive for MCT4. An MCT4 stromal staining score of low or high was given if < 30% or equal or greater than 30% of stromal cells stained positive for MCT4.

TOMM20, LDH-B staining as well as Ki-67 staining was also performed.

Cytochrome C oxidase (COX)/complex IV activity staining. Cryostat sections (8 μm) were prepared from HNSCC tissue samples that had been stored at -80°C until use. For the COX activity staining, frozen sections were brought to room temperature, washed for 5 min with 25 mM sodium phosphate buffer, pH 7.4 and then incubated for 1.5 and 2 h at 37°C with the COX incubation mixture as previously described.[92-94] The COX solution consisted of 10 mg cytochrome C, 10 mg 3,3'-diaminobenzidine tetrahydrochloride hydrate and 2 mg catalase (all components from Sigma-Aldrich) dissolved in 10 ml of 25 mM sodium phosphate buffer. The solution was filtered after preparation and the pH was adjusted to 7.2–7.4 with 1 N NaOH. Sections were counterstained with hematoxylin.

Statistical analysis. Data was analyzed using SAS 9.3. Fisher's exact test was used for assessment of association between MCT4 expression and pathologic variables including lymphovascular

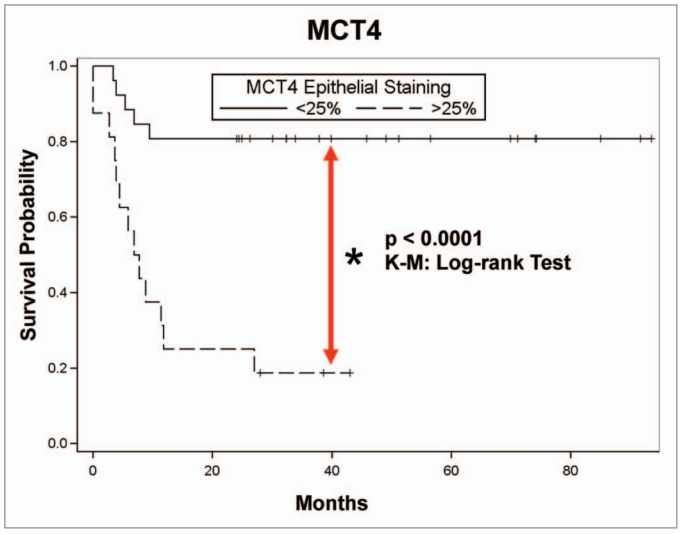

Figure 12. Epithelial MCT4 is a negative prognostic marker in HNSCC: Kaplan-Meier analysis and disease-free survival (DFS). Kaplan-Meier survival curves are shown for the 40 subjects analyzed. Note that higher levels of epithelial MCT4 expression are significantly associated with lower DFS (higher tumor recurrence; p = 0.0001; log-rank test).

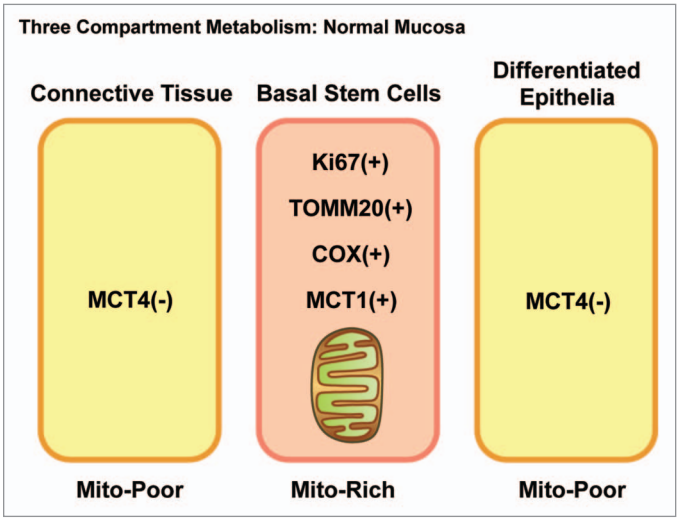

Figure 13. Three-compartment metabolism in normal mucosa. Note that in normal mucosa, three morphological and metabolic compartments can be distinguished. The basal stem cell layer is hyper-proliferative (Ki-67+), mitochondrial-rich (TOMM20+/COX+) and uses mitochondrial fuels (MCT1+). In contrast, the underlying connective tissue and the differentiated epithelial cells are non-proliferative and mitochondrial-poor. Importantly, all three compartments are MCT4-negative.

(LVI) or perineural invasion (PNI). Spearman's rank-order correlation was used for association of the MCT4 staining scores with each other and with the nodal and pathologic staging variables. Wilcoxon-Mann-Whitney test was used for association of MCT4 and maximum standard uptake value (SUV) on ^{18}Fluoro-2-Deoxy-Glucose (^{18}FDG) PET/CT. The distribution of disease-free survival (DFS) was estimated using the Kaplan-Meier method and groups were compared using the log-rank test. Cox proportional hazards regression was used to calculate adjusted estimates of differences in DFS. For all DFS analysis, an event is defined as a recurrence or a death. A p value < 0.05 was considered statistically significant. Subjects who were lost to follow-up are considered censored.

Disclosure of Potential Conflicts of Interest

No potential conflicts of interest were disclosed.

Acknowledgments

Statistical analysis was performed by Benjamin Leiby and Edward Pequignot, Division of Biostatistics Thomas Jefferson University.

U.E.M. was supported by a Young Investigator Award from the Margaret Q. Landenberger Research Foundation. Funds were also contributed by the Margaret Q. Landenberger Research Foundation (to M.P.L.). Also, these developments were made possible through the resources of Thomas Jefferson University.

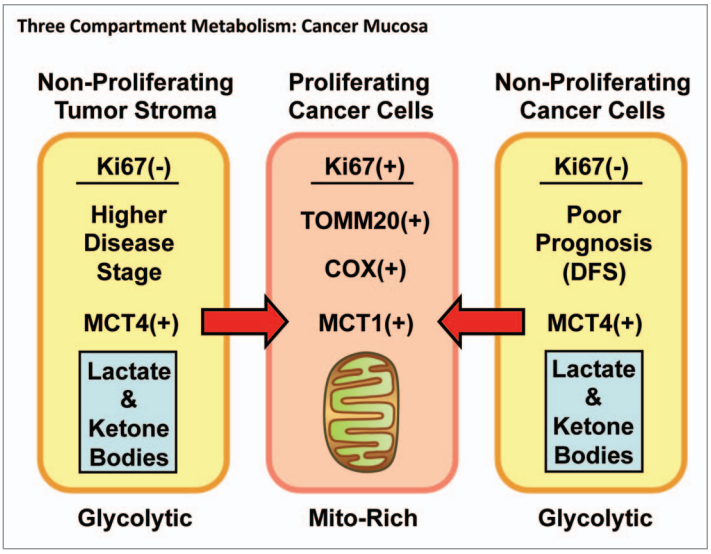

Figure 14. Three-compartment metabolism in HNSCC tumors. Note that in tumor tissue, three morphological and metabolic compartments could be identified. The poorly differentiated cancer cells are hyper-proliferative (Ki-67+), mitochondrial-rich (TOMM20+/COX+) and use mitochondrial fuels (MCT1+). In contrast, the tumor stroma and well-differentiated cancer cells are non-proliferative and mitochondrial-poor. However, in a subset of patients, both of these non-proliferating compartments are MCT4-positive, resulting in a higher disease stage or lower disease-free survival (DFS). MCT4 is a marker of oxidative stress and mitochondrial dysfunction, resulting in increased L-lactate and ketone body production, as well as export into the microenvironment. Thus, MCT1/MCT4 expression drives metabolic symbiosis in head and neck cancers.

References

1. Schmitz S, Machiels JP. Molecular biology of squamous cell carcinoma of the head and neck: relevance and therapeutic implications. Expert Rev Anticancer Ther 2010; 10:1471-84; PMID:20836682; http://dx.doi.org/10.1586/era.10.115
2. Lunt SY, Vander Heiden MG. Aerobic glycolysis: meeting the metabolic requirements of cell proliferation. Annu Rev Cell Dev Biol 2011; 27:441-64; PMID:21985671; http://dx.doi.org/10.1146/annurev-cellbio-092910-154237
3. Vander Heiden MG, Cantley LC, Thompson CB. Understanding the Warburg effect: the metabolic requirements of cell proliferation. Science 2009; 324:1029-33; PMID:19460998; http://dx.doi.org/10.1126/science.1160809
4. Moreno-Sánchez R, Rodríguez-Enríquez S, Marín-Hernández A, Saavedra E. Energy metabolism in tumor cells. FEBS J 2007; 274:1393-418; PMID:17302740; http://dx.doi.org/10.1111/j.1742-4658.2007.05686.x
5. Fantin VR, St-Pierre J, Leder P. Attenuation of LDH-A expression uncovers a link between glycolysis, mitochondrial physiology, and tumor maintenance. Cancer Cell 2006; 9:425-34; PMID:16766262; http://dx.doi.org/10.1016/j.ccr.2006.04.023
6. Sonveaux P, Végran F, Schroeder T, Wergin MC, Verrax J, Rabbani ZN, et al. Targeting lactate-fueled respiration selectively Kills hypoxic tumor cells in mice. J Clin Invest 2008; 118:3930-42; PMID:19033663
7. Zu XL, Guppy M. Cancer metabolism: facts, fantasy, and fiction. Biochem Biophys Res Commun 2004; 313:459-65; PMID:14697210; http://dx.doi.org/10.1016/j.bbrc.2003.11.136
8. Hanahan D, Weinberg RA. Hallmarks of cancer: the next generation. Cell 2011; 144:646-74; PMID:21376230; http://dx.doi.org/10.1016/j.cell.2011.02.013
9. Bellance N, Lestienne P, Rossignol R. Mitochondria: from bioenergetics to the metabolic regulation of carcinogenesis. Front Biosci 2009; 14:4015-34; PMID:19273331
10. Martinez-Outschoorn UE, Sotgia F, Lisanti MP. Power surge: supporting cells "fuel" cancer cell mitochondria. Cell Metab 2012; 15:4-5; PMID:22225869; http://dx.doi.org/10.1016/j.cmet.2011.12.011.
11. Paget S. The distribution of secondary growths in cancer of the breast. 1889. Cancer Metastasis Rev 1989; 8:98-101; PMID:2673568
12. Pavlides S, Whitaker-Menezes D, Castello-Cros R, Flomenberg N, WitKiewicz AK, Frank PG, et al. The reverse Warburg effect: aerobic glycolysis in cancer-associated fibroblasts and the tumor stroma. Cell Cycle 2009; 8:3984-4001; PMID:19923890; http://dx.doi.org/10.4161/cc.8.23.10238
13. Martinez-Outschoorn UE, Lin Z, Trimmer C, Flomenberg N, Wang C, Pavlides S, et al. Cancer cells metabolically "fertilize" the tumor microenvironment with hydrogen peroxide, driving the Warburg effect: implications for PET imaging of human tumors. Cell Cycle 2011; 10:2504-20; PMID:21778829; http://dx.doi.org/10.4161/cc.10.15.16585
14. Bonuccelli G, Tsirigos A, Whitaker-Menezes D, Pavlides S, Pestell RG, Chiavarina B, et al. Ketones and lactate "fuel" tumor growth and metastasis: Evidence that epithelial cancer cells use oxidative mitochondrial metabolism. Cell Cycle 2010; 9:3506-14; PMID:20818174; http://dx.doi.org/10.4161/cc.9.17.12731
15. Martinez-Outschoorn UE, Goldberg A, Lin Z, Ko YH, Flomenberg N, Wang C, et al. Anti-estrogen resistance in breast cancer is induced by the tumor microenvironment and can be overcome by inhibiting mitochondrial function in epithelial cancer cells. Cancer Biol Ther 2011; 12:924-38; PMID:22041887; http://dx.doi.org/10.4161/cbt.12.10.17780
16. Martinez-Outschoorn UE, Pestell RG, Howell A, TykocinsKi ML, Nagajyothi F, Machado FS, et al. Energy transfer in "parasitic" cancer metabolism: mitochondria are the powerhouse and Achilles' heel of tumor cells. Cell Cycle 2011; 10:4208-16; PMID:22033146; http://dx.doi.org/10.4161/cc.10.24.18487
17. WitKiewicz AK, Whitaker-Menezes D, Dasgupta A, Philp NJ, Lin Z, Gandara R, et al. Using the "reverse Warburg effect" to identify high-risk breast cancer patients: stromal MCT4 predicts poor clinical outcome in triple-negative breast cancers. Cell Cycle 2012; 11:1108-17; PMID:22313602; http://dx.doi.org/10.4161/cc.11.6.19530
18. Walenta S, Salameh A, Lyng H, Evensen JF, Mitze M, Rofstad EK, et al. Correlation of high lactate levels in head and neck tumors with incidence of metastasis. Am J Pathol 1997; 150:409-15; PMID:9033256
19. Brizel DM, Schroeder T, Scher RL, Walenta S, Clough RW, Dewhirst MW, et al. Elevated tumor lactate concentrations predict for an increased risk of metastases in head-and-neck cancer. Int J Radiat Oncol Biol Phys 2001; 51:349-53; PMID:11567808; http://dx.doi.org/10.1016/S0360-3016(01)01630-3
20. Tripathi P, Kamarajan P, Somashekar BS, MacKinnon N, Chinnaiyan AM, Kapila YL, et al. Delineating metabolic signatures of head and neck squamous cell carcinoma: phospholipase A2, a potential therapeutic target. Int J Biochem Cell Biol 2012; 44:1852-61; PMID:22743333; http://dx.doi.org/10.1016/j.biocel.2012.06.025

21. Sandulache VC, Ow TJ, Pickering CR, Frederick MJ, Zhou G, Fokt I, et al. Glucose, not glutamine, is the dominant energy source required for proliferation and survival of head and neck squamous carcinoma cells. Cancer 2011; 117:2926-38; PMID:21692052; http://dx.doi.org/10.1002/cncr.25868
22. Lee SY, Jeon HM, Ju MK, Kim CH, Yoon G, Han SI, et al. Wnt/Snail signaling regulates cytochrome C oxidase and glucose metabolism. Cancer Res 2012; 72:3607-17; PMID:22637725; http://dx.doi.org/10.1158/0008-5472.CAN-12-0006
23. Fontanesi F, Soto IC, Horn D, Barrientos A. Assembly of mitochondrial cytochrome c-oxidase, a complicated and highly regulated cellular process. Am J Physiol Cell Physiol 2006; 291:C1129-47; PMID:16760263; http://dx.doi.org/10.1152/ajpcell.00233.2006
24. Rustin P, Chretien D, Bourgeron T, Gérard B, Rötig A, Saudubray JM, et al. Biochemical and molecular investigations in respiratory chain deficiencies. Clin Chim Acta 1994; 228:35-51; PMID:7955428; http://dx.doi.org/10.1016/0009-8981(94)90055-8
25. King MP, Koga Y, Davidson M, Schon EA. Defects in mitochondrial protein synthesis and respiratory chain activity segregate with the tRNA(Leu(UUR)) mutation associated with mitochondrial myopathy, encephalopathy, lactic acidosis, and strokelike episodes. Mol Cell Biol 1992; 12:480-90; PMID:1732728
26. Nonaka I, Koga Y, Shikura K, Kobayashi M, Sugiyama N, OKino E, et al. Muscle pathology in cytochrome c oxidase deficiency. Acta Neuropathol 1988; 77:152-60; PMID:2852426
27. Papadopoulou LC, Sue CM, Davidson MM, Tanji K, Nishino I, Sadlock JE, et al. Fatal infantile cardioencephalomyopathy with COX deficiency and mutations in SCO2, a COX assembly gene. Nat Genet 1999; 23:333-7; PMID:10545952; http://dx.doi.org/10.1038/15513
28. Borthwick GM, Johnson MA, Ince PG, Shaw PJ, Turnbull DM. Mitochondrial enzyme activity in amyotrophic lateral sclerosis: implications for the role of mitochondria in neuronal cell death. Ann Neurol 1999; 46:787-90; PMID:10553999; http://dx.doi.org/10.1002/1531-8249(199911)46:5<787::AID-ANA17>3.0.CO;2-8
29. Ross JM. Visualization of mitochondrial respiratory function using cytochrome c oxidase/succinate dehydrogenase (COX/SDH) double-labeling histochemistry. J Vis Exp 2011:e3266; PMID:22143245
30. Yano M, Terada K, Mori M. Mitochondrial import receptors Tom20 and Tom22 have chaperone-like activity. J Biol Chem 2004; 279:10808-13; PMID:14699115; http://dx.doi.org/10.1074/jbc.M311710200
31. Yano M, Kanazawa M, Terada K, Takeya M, Hoogenraad N, Mori M. Functional analysis of human mitochondrial receptor Tom20 for protein import into mitochondria. J Biol Chem 1998; 273:26844-51; PMID:9756929; http://dx.doi.org/10.1074/jbc.273.41.26844
32. Wurm CA, Neumann D, Lauterbach MA, Harke B, Egner A, Hell SW, et al. Nanoscale distribution of mitochondrial import receptor Tom20 is adjusted to cellular conditions and exhibits an inner-cellular gradient. Proc Natl Acad Sci USA 2011; 108:13546-51; PMID:21799113; http://dx.doi.org/10.1073/pnas.1107553108
33. Halestrap AP, Price NT. The proton-linked monocarboxylate transporter (MCT) family: structure, function and regulation. Biochem J 1999; 343:281-99; PMID:10510291; http://dx.doi.org/10.1042/0264-6021:3430281
34. Sonveaux P, Copetti T, De Saedeleer CJ, Végran F, Verrax J, Kennedy KM, et al. Targeting the lactate transporter MCT1 in endothelial cells inhibits lactate-induced HIF-1 activation and tumor angiogenesis. PLoS ONE 2012; 7:e33418; PMID:22428047; http://dx.doi.org/10.1371/journal.pone.0033418
35. Bonen A. The expression of lactate transporters (MCT1 and MCT4) in heart and muscle. Eur J Appl Physiol 2001; 86:6-11; PMID:11820324; http://dx.doi.org/10.1007/s004210100516
36. Ganapathy V, Thangaraju M, Prasad PD. Nutrient transporters in cancer: relevance to Warburg hypothesis and beyond. Pharmacol Ther 2009; 121:29-40; PMID:18992769; http://dx.doi.org/10.1016/j.pharmthera.2008.09.005
37. Dimmer KS, Friedrich B, Lang F, Deitmer JW, Bröer S. The low-affinity monocarboxylate transporter MCT4 is adapted to the export of lactate in highly glycolytic cells. Biochem J 2000; 350:219-27; PMID:10926847; http://dx.doi.org/10.1042/0264-6021:3500219
38. Brooks GA. Cell-cell and intracellular lactate shuttles. J Physiol 2009; 587:5591-600; PMID:19805739; http://dx.doi.org/10.1113/jphysiol.2009.178350
39. Ullah MS, Davies AJ, Halestrap AP. The plasma membrane lactate transporter MCT4, but not MCT1, is up-regulated by hypoxia through a HIF-1alpha-dependent mechanism. J Biol Chem 2006; 281:9030-7; PMID:16452478; http://dx.doi.org/10.1074/jbc.M511397200
40. Nordsmark M, Bentzen SM, Rudat V, Brizel D, Lartigau E, Stadler P, et al. Prognostic value of tumor oxygenation in 397 head and neck tumors after primary radiation therapy. An international multi-center study. Radiother Oncol 2005; 77:18-24; PMID:16098619; http://dx.doi.org/10.1016/j.radonc.2005.06.038
41. Kaanders JH, Wijffels KI, Marres HA, Ljungkvist AS, Pop LA, van den Hoogen FJ, et al. Pimonidazole binding and tumor vascularity predict for treatment outcome in head and neck cancer. Cancer Res 2002; 62:7066-74; PMID:12460928
42. Valavanidis A, Vlachogianni T, FiotaKis K. Tobacco smoke: involvement of reactive oxygen species and stable free radicals in mechanisms of oxidative damage, carcinogenesis and synergistic effects with other respirable particles. Int J Environ Res Public Health 2009; 6:445-62; PMID:19440393; http://dx.doi.org/10.3390/ijerph6020445
43. Valavanidis A, Vlachogianni T, FiotaKis C. 8-hydroxy-2'-deoxyguanosine (8-OHdG): A critical biomarker of oxidative stress and carcinogenesis. J Environ Sci Health C Environ Carcinog Ecotoxicol Rev 2009; 27:120-39; PMID:19412858; http://dx.doi.org/10.1080/10590500902885684
44. Bahar G, Feinmesser R, Shpitzer T, Popovtzer A, Nagler RM. Salivary analysis in oral cancer patients: DNA and protein oxidation, reactive nitrogen species, and antioxidant profile. Cancer 2007; 109:54-9; PMID:17099862; http://dx.doi.org/10.1002/cncr.22386
45. Kumar A, Pant MC, Singh HS, Khandelwal S. Assessment of the redox profile and oxidative DNA damage (8-OHdG) in squamous cell carcinoma of head and neck. J Cancer Res Ther 2012; 8:254-9; PMID:22842371; http://dx.doi.org/10.4103/0973-1482.98980
46. Zha X, Wang F, Wang Y, He S, Jing Y, Wu X, et al. Lactate dehydrogenase B is critical for hyperactive mTOR-mediated tumorigenesis. Cancer Res 2011; 71:13-8; PMID:21199794; http://dx.doi.org/10.1158/0008-5472.CAN-10-1668
47. Jones RG, Thompson CB. Tumor suppressors and cell metabolism: a recipe for cancer growth. Genes Dev 2009; 23:537-48; PMID:19270154; http://dx.doi.org/10.1101/gad.1756509
48. Härle-Bachor C, Boukamp P. Telomerase activity in the regenerative basal layer of the epidermis inhuman sKin and in immortal and carcinoma-derived sKin keratinocytes. Proc Natl Acad Sci USA 1996; 93:6476-81; PMID:8692840; http://dx.doi.org/10.1073/pnas.93.13.6476
49. Bojovic B, Crowe DL. Telomere dysfunction promotes metastasis in a TERC null mouse model of head and neck cancer. Mol Cancer Res 2011; 9:901-13; PMID:21593138; http://dx.doi.org/10.1158/1541-7786.MCR-10-0345
50. Blackburn EH. Telomere states and cell fates. Nature 2000; 408:53-6; PMID:11081503; http://dx.doi.org/10.1038/35040500
51. Jensen KB, Jones J, Watt FM. A stem cell gene expression profile of human squamous cell carcinomas. Cancer Lett 2008; 272:23-31; PMID:18657901; http://dx.doi.org/10.1016/j.canlet.2008.06.014
52. Martinez-Outschoorn UE, Prisco M, Ertel A, Tsirigos A, Lin Z, Pavlides S, et al. Ketones and lactate increase cancer cell "stemness," driving recurrence, metastasis and poor clinical outcome in breast cancer: achieving personalized medicine via Metabolo-Genomics. Cell Cycle 2011; 10:1271-86; PMID:21512313; http://dx.doi.org/10.4161/cc.10.8.15330
53. Martinez-Outschoorn UE, Balliet RM, Lin Z, Whitaker-Menezes D, Howell A, Sotgia F, et al. Hereditary ovarian cancer and two-compartment tumor metabolism: epithelial loss of BRCA1 induces hydrogen peroxide production, driving oxidative stress and NFκB activation in the tumor stroma. Cell Cycle 2012; 11:4152-66; PMID:23047606; http://dx.doi.org/10.4161/cc.22226
54. Martinez-Outschoorn UE, Balliet R, Lin Z, Whitaker-Menezes D, Birbe RC, Bombonati A, et al. BRCA1 mutations drive oxidative stress and glycolysis in the tumor microenvironment: implications for breast cancer prevention with antioxidant therapies. Cell Cycle 2012; 11:4402-13; PMID:23172369; http://dx.doi.org/10.4161/cc.22776
55. Nieman KM, Kenny HA, Penicka CV, Ladanyi A, Buell-Gutbrod R, Zillhardt MR, et al. Adipocytes promote ovarian cancer metastasis and provide energy for rapid tumor growth. Nat Med 2011; 17:1498-503; PMID:22037646; http://dx.doi.org/10.1038/nm.2492
56. KoukouraKis MI, GiatromanolaKi A, Harris AL, Sivridis E. Comparison of metabolic pathways between cancer cells and stromal cells in colorectal carcinomas: a metabolic survival role for tumor-associated stroma. Cancer Res 2006; 66:632-7; PMID:16423989; http://dx.doi.org/10.1158/0008-5472.CAN-05-3260
57. Fiaschi T, Marini A, Giannoni E, Taddei ML, Gandellini P, De Donatis A, et al. Reciprocal metabolic reprogramming through lactate shuttle coordinately influences tumor-stroma interplay. Cancer Res 2012; 72:5130-40; PMID:22850421; http://dx.doi.org/10.1158/0008-5472.CAN-12-1949
58. GiatromanolaKi A, KoukouraKis MI, Koutsopoulos A, Mendrinos S, Sivridis E. The metabolic interactions between tumor cells and tumor-associated stroma (TAS) in prostatic cancer. Cancer Biol Ther 2012; 13:1284-9; PMID:22895074; http://dx.doi.org/10.4161/cbt.21785
59. Weinberg F, Hamanaka R, Wheaton WW, Weinberg S, Joseph J, Lopez M, et al. Mitochondrial metabolism and ROS generation are essential for Kras-mediated tumorigenicity. Proc Natl Acad Sci USA 2010; 107:8788-93; PMID:20421486; http://dx.doi.org/10.1073/pnas.1003428107
60. Zhdanov VP. Stochastic model of the formation of cancer metastases via cancer stem cells. Eur Biophys J 2008; 37:1329-34; PMID:18463859; http://dx.doi.org/10.1007/s00249-008-0341-9
61. Skelton MS, Kremer DE, Smith EW, Gladden LB. Lactate influx into red blood cells from trained and untrained human subjects. Med Sci Sports Exerc 1998; 30:536-42; PMID:9565935; http://dx.doi.org/10.1097/00005768-199804000-00011
62. Gladden LB. Lactate metabolism: a new paradigm for the third millennium. J Physiol 2004; 558:5-30; PMID:15131240; http://dx.doi.org/10.1113/jphysiol.2003.058701

63. Pinheiro C, Albergaria A, Paredes J, Sousa B, Dufloth R, Vieira D, et al. Monocarboxylate transporter 1 is up-regulated in basal-like breast carcinoma. Histopathology 2010; 56:860-7; PMID:20636790; http://dx.doi.org/10.1111/j.1365-2559.2010.03560.x
64. Semenza GL. Tumor metabolism: cancer cells give and take lactate. J Clin Invest 2008; 118:3835-7; PMID:19033652
65. Fang J, Quinones QJ, Holman TL, Morowitz MJ, Wang Q, Zhao H, et al. The H+-linked monocarboxylate transporter (MCT1/SLC16A1): a potential therapeutic target for high-risk neuroblastoma. Mol Pharmacol 2006; 70:2108-15; PMID:17000864; http://dx.doi.org/10.1124/mol.106.026245
66. Jones NP, Schulze A. Targeting cancer metabolism--aiming at a tumour's sweet-spot. Drug Discov Today 2012; 17:232-41; PMID:22207221; http://dx.doi.org/10.1016/j.drudis.2011.12.017
67. Vitale-Cross L, Molinolo AA, Martin D, Younis RH, Maruyama T, Patel V, et al. Metformin prevents the development of oral squamous cell carcinomas from carcinogen-induced premalignant lesions. Cancer Prev Res (Phila) 2012; 5:562-73; PMID:22467081; http://dx.doi.org/10.1158/1940-6207.CAPR-11-0502
68. Haddad RI, Shin DM. Recent advances in head and neck cancer. N Engl J Med 2008; 359:1143-54; PMID:18784104; http://dx.doi.org/10.1056/NEJMra0707975
69. Kroemer G, Pouyssegur J. Tumor cell metabolism: cancer's Achilles' heel. Cancer Cell 2008; 13:472-82; PMID:18538731; http://dx.doi.org/10.1016/j.ccr.2008.05.005
70. Rademakers SE, Lok J, van der Kogel AJ, Bussink J, Kaanders JH. Metabolic markers in relation to hypoxia; staining patterns and colocalization of pimonidazole, HIF-1α, CAIX, LDH-5, GLUT-1, MCT1 and MCT4. BMC Cancer 2011; 11:167; PMID:21569415; http://dx.doi.org/10.1186/1471-2407-11-167
71. Martinez-Outschoorn UE, Balliet RM, Rivadeneira DB, Chiavarina B, Pavlides S, Wang C, et al. Oxidative stress in cancer-associated fibroblasts drives tumor-stroma co-evolution: A new paradigm for understanding tumor metabolism, the field effect and genomic instability in cancer cells. Cell Cycle 2010; 9:3256-76; PMID:20814239; http://dx.doi.org/10.4161/cc.9.16.12553
72. Whitaker-Menezes D, Martinez-Outschoorn UE, Lin Z, Ertel A, Flomenberg N, WitKiewicz AK, et al. Evidence for a stromal-epithelial "lactate shuttle" in human tumors: MCT4 is a marker of oxidative stress in cancer-associated fibroblasts. Cell Cycle 2011; 10:1772-83; PMID:21558814; http://dx.doi.org/10.4161/cc.10.11.15659
73. Haas RH, Parikh S, Falk MJ, Saneto RP, Wolf NI, Darin N, et al.; Mitochondrial Medicine Society's Committee on Diagnosis. The in-depth evaluation of suspected mitochondrial disease. Mol Genet Metab 2008; 94:16-37; PMID:18243024; http://dx.doi.org/10.1016/j.ymgme.2007.11.018
74. Ben Sahra I, Tanti JF, Bost F. The combination of metformin and 2 deoxyglucose inhibits autophagy and induces AMPK-dependent apoptosis in prostate cancer cells. Autophagy 2010; 6; PMID:20559023; http://dx.doi.org/10.4161/auto.6.5.12434
75. Juweid ME, Cheson BD. Positron-emission tomography and assessment of cancer therapy. N Engl J Med 2006; 354:496-507; PMID:16452561; http://dx.doi.org/10.1056/NEJMra050276.
76. AAssar OS, Fischbein NJ, Caputo GR, Kaplan MJ, Price DC, Singer MI, et al.; OS AA. Metastatic head and neck cancer: role and usefulness of FDG PET in locating occult primary tumors. Radiology 1999; 210:177-81; PMID:9885604
77. Subramaniam RM, Truong M, Peller P, Sakai O, Mercier G. Fluorodeoxyglucose-positron-emission tomography imaging of head and neck squamous cell cancer. AJNR Am J Neuroradiol 2010; 31:598-604; PMID:19910448; http://dx.doi.org/10.3174/ajnr.A1760
78. Machtay M, Natwa M, Andrel J, Hyslop T, Anne PR, Lavarino J, et al. Pretreatment FDG-PET standardized uptake value as a prognostic factor for outcome in head and neck cancer. Head Neck 2009; 31:195-201; PMID:19107945; http://dx.doi.org/10.1002/hed.20942
79. Halfpenny W, Hain SF, Biassoni L, Maisey MN, Sherman JA, McGurk M. FDG-PET. A possible prognostic factor in head and neck cancer. Br J Cancer 2002; 86:512-6; PMID:11870529; http://dx.doi.org/10.1038/sj.bjc.6600114
80. Schwartz DL, Rajendran J, Yueh B, Coltrera MD, Leblanc M, Eary J, et al. FDG-PET prediction of head and neck squamous cell cancer outcomes. Arch Otolaryngol Head Neck Surg 2004; 130:1361-7; PMID:15611393; http://dx.doi.org/10.1001/archotol.130.12.1361
81. Nakajo M, Nakajo M, Kajiya Y, Tani A, Kamiyama T, Yonekura R, et al. FDG PET/CT and diffusion-weighted imaging of head and neck squamous cell carcinoma: comparison of prognostic significance between primary tumor standardized uptake value and apparent diffusion coefficient. Clin Nucl Med 2012; 37:475-80; PMID:22475897; http://dx.doi.org/10.1097/RLU.0b013e318248524a
82. Minn H, Lapela M, Klemi PJ, Grénman R, LesKinen S, Lindholm P, et al. Prediction of survival with fluorine-18-fluoro-deoxyglucose and PET in head and neck cancer. J Nucl Med 1997; 38:1907-11; PMID:9430467
83. Slaughter DP. Multicentric origin of intraoral carcinoma. Surgery 1946; 20:133-46; PMID:20992244
84. Tabor MP, Brakenhoff RH, Ruijter-Schippers HJ, Van Der Wal JE, Snow GB, Leemans CR, et al. Multiple head and neck tumors frequently originate from a single preneoplastic lesion. Am J Pathol 2002; 161:1051-60; PMID:12213734; http://dx.doi.org/10.1016/S0002-9440(10)64266-6
85. Tabor MP, Brakenhoff RH, Ruijter-Schippers HJ, Kummer JA, Leemans CR, Braakhuis BJ. Genetically altered fields as origin of locally recurrent head and neck cancer: a retrospective study. Clin Cancer Res 2004; 10:3607-13; PMID:15173066; http://dx.doi.org/10.1158/1078-0432.CCR-03-0632
86. Tsui IF, Garnis C, Poh CF. A dynamic oral cancer field: unraveling the underlying biology and its clinical implication. Am J Surg Pathol 2009; 33:1732-8; PMID:19858864; http://dx.doi.org/10.1097/PAS.0b013e3181b669c2
87. Brockton N, Dort J, Lau H, Hao D, Brar S, Klimowicz A, et al. High stromal carbonic anhydrase IX expression is associated with decreased survival in P16-negative head-and-neck tumors. Int J Radiat Oncol Biol Phys 2011; 80:249-57; PMID:21300470; http://dx.doi.org/10.1016/j.ijrobp.2010.11.059
88. Brockton NT, Klimowicz AC, Bose P, Petrillo SK, Konno M, Rudmik L, et al. High stromal carbonic anhydrase IX expression is associated with nodal metastasis and decreased survival in patients with surgically-treated oral cavity squamous cell carcinoma. Oral Oncol 2012; 48:615-22; PMID:22366443; http://dx.doi.org/10.1016/j.oraloncology.2012.01.018
89. Califano J, van der Riet P, Westra W, Nawroz H, Clayman G, Piantadosi S, et al. Genetic progression model for head and neck cancer: implications for field cancerization. Cancer Res 1996; 56:2488-92; PMID:8653682
90. Guppy M, Leedman P, Zu X, Russell V. Contribution by different fuels and metabolic pathways to the total ATP turnover of proliferating MCF-7 breast cancer cells. Biochem J 2002; 364:309-15; PMID:11988105
91. Gallagher SM, Castorino JJ, Wang D, Philp NJ. Monocarboxylate transporter 4 regulates maturation and traffickIng of CD147 to the plasma membrane in the metastatic breast cancer cell line MDA-MB-231. Cancer Res 2007; 67:4182-9; PMID:17483329; http://dx.doi.org/10.1158/0008-5472.CAN-06-3184
92. Tanji K, Bonilla E. Light microscopic methods to visualize mitochondria on tissue sections. Methods 2008; 46:274-80; PMID:18929660; http://dx.doi.org/10.1016/j.ymeth.2008.09.027
93. Mahad DJ, Ziabreva I, Campbell G, Laulund F, Murphy JL, Reeve AK, et al. Detection of cytochrome c oxidase activity and mitochondrial proteins in single cells. J Neurosci Methods 2009; 184:310-9; PMID:19723540; http://dx.doi.org/10.1016/j.jneumeth.2009.08.020
94. Whitaker-Menezes D, Martinez-Outschoorn UE, Flomenberg N, Birbe RC, WitKiewicz AK, Howell A, et al. Hyperactivation of oxidative mitochondrial metabolism in epithelial cancer cells in situ: visualizing the therapeutic effects of metformin in tumor tissue. Cell Cycle 2011; 10:4047-64; PMID:22134189; http://dx.doi.org/10.4161/cc.10.23.18151